Lowfrequency instabilities in the highpressure regime of Penning discharges

S. K. Guharay, S. N. SenGupta, and M. R. Gupta

Citation: J. Appl. Phys. **49**, 5809 (1978); doi: 10.1063/1.324596
View online: http://dx.doi.org/10.1063/1.324596
View Table of Contents: http://jap.aip.org/resource/1/JAPIAU/v49/i12
Published by the AIP Publishing LLC.

Low-frequency instabilities in the high-pressure regime of Penning discharges

S. K. Guharay and S. N. SenGupta

Saha Institute of Nuclear Physics, Calcutta-700009, India

M. R. Gupta

Centre of Advanced Studies in Applied Mathematics, Calcutta University, Calcutta-700009, India
(Received 6 December 1977; accepted for publication 8 March 1978)

A general dispersion relation for the rotationally symmetric ($m=0$) and asymmetric ($m\neq 0$) low-frequency waves has been delineated, utilizing a dimensional treatment as done by Hoh, for a high-pressure ($p\sim 10^{-2}$ Torr) Penning discharge having gradients (radial) of ion density, plasma potential, and electron temperature. The present analysis is found to be very helpful for investigating the role of the temperature gradient in exciting various modes; here, a positive temperature gradient has been found to have a destabilizing influence in general. The theoretical predictions of the growth condition and the frequency of the instability have been found to agree well with the present experimental observation of an $m=0$ mode. Further, an experiment on the suppression of this instability has been carried out for understanding the excitation mechanism.

PACS numbers: 52.35.Py, 52.80.Sm, 52.25.Lp, 52.70.Ds

I. INTRODUCTION

Low-frequency instabilities in a Penning discharge (PIG) have been investigated both theoretically and experimentally by numerous workers, e.g., Hoh,[1] Bingham,[2] Thomassen,[3] Hooper,[4] etc. The theoretical analyses of Hoh,[1] Bingham,[2] etc., reveal that an $m=1$ mode is the least stable in a conventional Penning discharge at high gas pressures when there exist radial ion density (n_i) and plasma potential (V_s) gradients. But, in experimental situations this is not always observed. Thomassen[3] observed the $m=3$ mode to be the least stable, while Hooper[4] found the least stable mode to be the $m=2$ mode. Kaganskii *et al.*[5] observed a rotationally symmetric mode ($m=0$) and interpreted the instability frequency to correspond to the convective-flow instability as formulated by Kadomtsev.[6] Ecker *et al.*[7] have shown theoretically that an $m=0$ mode instability can occur due to the coupling of density and temperature disturbances in a weakly ionized plasma column. However, the onset of a particular mode in a Penning discharge is found to be highly dependent on the explicit behavior of various parameters, e.g., gas pressure, magnetic field, discharge current, etc., and also of the geometry.

In the present experimental investigation, a cold-cathode PIG system has been operated in the high-pressure regime ($p\sim 10^{-2}$ Torr) with the degree of ionization less than 0.1% (i.e., weakly ionized plasma) and observation of the low-frequency waves have been carried out. Here the interesting feature is that a strong rotationally symmetric mode ($m=0$) has been observed at low magnetic fields when there exists a positive radial electron-temperature gradient ($\partial T_e/\partial r$). Such a mode, driven by $\partial T_e/\partial r$ has not been reported by the previous workers. Further, this mode ($m=0$) has been stabilized by reducing the aforesaid gradient to a negligible value. It is, therefore, felt that the role of the electron-temperature gradient needs to be incorporated in the earlier theories for a proper understanding of the observed instability. Such a gradient has also been observed by several workers (Chen,[8] Horikoshi *et al.*,[9] etc.) in a PIG system. In a review by Mikhailovskii[10] on plasma instabilities, the importance of the temperature distribution has been enunciated explicitly. Moreover, Pekárek *et al.*[11] have indicated that the temperature gradient has a strong influence on the diffusion of electrons in a weakly ionized plasma and, as a consequence, this gradient is likely to contribute significantly to the excitation mechanism of instabilities in the plasma.

Here attempts have been made to analyze theoretically the low-frequency instabilities, without restricting the mode number, that may come about in a high-pressure PIG discharge in the presence of the gradients of n_i, V_s, and T_e and also the occurence of the $m=0$ mode has been investigated theoretically to support the observed phenomenon. The theoretical procedure is based on the dimensional analysis as has been done by Hoh.[1] Although it is an approximative method, much significant qualitative information can be obtained with its help; otherwise, it becomes very difficult to solve the complicated differential equations anaytically. Klan[12] has also applied this dimensional analysis in investigating the low-frequency temperature perturbations in a PIG discharge.

The theoretical considerations of the present problem are given in Sec. II, experimental results and discussion are in Sec. III, and the conclusions are in Sec. IV.

II. THEORETICAL CONSIDERATIONS

A. General method

The equations of motion of electrons and ions in a weakly ionized plasma are

$$m_e n_e \frac{d\mathbf{v}_e}{dt} = -n_e e(-\nabla V + \mathbf{v}_e \times \mathbf{B}) - \nabla p_e - \mathbf{P}_{en} + \mathbf{R}_T, \tag{1}$$

 0021-8979/78/4912-5809$01.10

$$m_i n_i \frac{d\mathbf{v}_i}{dt} = n_i e(-\nabla V + \mathbf{v}_i \times \mathbf{B}) - p_i - \mathbf{P}_{in}, \tag{2}$$

where m corresponds to the mass, n the charge density, $\mathbf{v}$ the velocity, and p the kinetic pressure of electrons and ions as specified by the subscripts e and i, respectively. Here e and $V(\equiv V_s)$ stand for electronic charge and plasma potential, respectively. $\mathbf{P}_{en}$ and $\mathbf{P}_{in}$ represent the momentum transfer due to elastic collisions between electrons and neutrals and ions and neutrals, respectively, and these are given by

$$\mathbf{P}_{en} = m_e n_e(\mathbf{v}_e - \mathbf{v}_n)/\tau_{en}, \qquad \mathbf{P}_{in} = m_i n_i(\mathbf{v}_i - \mathbf{v}_n)/\tau_{in}, \tag{3}$$

where the τ's correspond to the mean collision times and $\mathbf{v}_n$ is the velocity of the neutrals. Here the contribution due to the interaction between the charged components is negligible. $\mathbf{R}_T$ in Eq. (1) denotes the thermal force on the electrons arising out of a radial electron-temperature gradient. This was not included in the earlier works mentioned above. The explicit form of $\mathbf{R}_T$ can be obtained following Braginskii[13] for $\omega_e \tau_{en} \gg 1$ as

$$\mathbf{R}_T = -3/2(n_e/\omega_e \tau_{en})\hat{b} \times \nabla T_e, \tag{4}$$

ω_e being the electron-cyclotron frequency and $\hat{b}$ the unit vector in the direction of the magnetic field $\mathbf{B}$. Since in the present situation electron-ion interactions are less frequent compared to the electron-neutral ones, its contribution in the thermal force term is neglected. The ions being cold in the present case, the contribution from the thermal force term in its equation of motion [Eq. (2)] is neglected.

To investigate the low-frequency oscillations, the inertial terms in Eqs. (1) and (2) are neglected. Also, the neutrals are assumed to be immobile and the quasineutrality condition $n \approx n_e \approx n_i$ is supposed to hold. Utilizing these conditions and the expressions in Eqs. (3) and (4), Eqs. (1) and (2) become

$$\frac{m_e n \mathbf{v}_e}{\tau_e} = ne(\nabla V + B\hat{b} \times \mathbf{v}_e) - T_e \nabla n - n \nabla T_e - 3/2 \frac{n\hat{b} \times \nabla T_e}{\omega_e \tau_e}, \tag{5}$$

$$\frac{m_i n \mathbf{v}_i}{\tau_i} = -ne(\nabla V + B\hat{b} \times \mathbf{v}_i) - T_i \nabla n, \tag{6}$$

respectively. Here $\tau_e \equiv \tau_{en}$ and $\tau_i \equiv \tau_{in}$ and the Boltzmann constant has been taken to be unity.

In a cylindrical coordinate system (r,θ,z) with the magnetic field in the z direction, the transverse components of $n\mathbf{v}_e$ and $n\mathbf{v}_i$ are

$$\begin{aligned} nv_{e\perp} &= -D_{e\perp} \nabla_\perp n + nb_{e\perp} \nabla_\perp V - D_{e\perp} \alpha_e(\hat{b} \times \nabla n)_\perp \\ &\quad + nb_{e\perp} \alpha_e(\hat{b} \times \nabla V)_\perp + (nb_{e\perp}/2e)\nabla_\perp T_e \\ &\quad - (nb_{e\perp})\, \alpha_e(\hat{b} \times \nabla T_e)_\perp, \\ nv_{i\perp} &= -D_{i\perp} \nabla_\perp n - nb_{i\perp} \nabla_\perp V \\ &\quad + D_{i\perp} \alpha_i(\hat{b} \times \nabla n)_\perp + nb_{i\perp} \alpha_i(\hat{b} \times \nabla V)_\perp \end{aligned} \tag{7}$$

and the components along the direction of the magnetic field are

$$nv_{ez} = nb_e \frac{\partial V}{\partial z} - D_e \frac{\partial n}{\partial z}, \tag{9}$$

$$nv_{iz} = -nb_i \frac{\partial V}{\partial z} - D_i \frac{\partial n}{\partial z}, \tag{10}$$

where the free-electron and ion mobilities are

$$b_e = e\tau_e/m_e \quad \text{and} \quad b_i = e\tau_i/m_i,$$

respectively, and the corresponding diffusion coefficients are

$$D_e = T_e b_e/e \quad \text{and} \quad D_i = T_i b_i/e.$$

The subscript $\perp$ in the mobility and diffusion terms in Eqs. (7) and (8) refers to division of the above expressions for b's and D's by $(1+\alpha_e^2)$ for electrons and $(1+\alpha_i^2)$ for ions where $\alpha_e = \omega_e \tau_e$ and $\alpha_i = \omega_i \tau_i$. In Eq. (7), the approximation $\alpha_e^2 \gg 1$ has been incorporated and this has been maintained throughout.

The equations of continuity for electrons and ions are

$$\frac{\partial n}{\partial t} + \operatorname{div}(n\mathbf{v}_e) = Zn, \qquad \frac{\partial n}{\partial t} + \operatorname{div}(n\mathbf{v}_i) = Zn, \tag{11}$$

where Z is the production rate of charged particles. Next in Eqs. (7)–(11) the density (n) and the potential (V) are replaced by its steady distributions and the fluctuating ones, having the following forms:

$$\begin{aligned} n &\to n + n_1 = n + n_1(r) \exp(\omega t + im\theta + ikz), \\ V &\to V + V_1 = V + V_1(r) \exp(\omega t + im\theta + ikz), \end{aligned} \tag{12}$$

where the suffix 1 corresponds to fluctuation, m the azimuthal mode number, and k the axial wave number. The real and imaginary parts of ω will convey the growth rate and the frequency of oscillation of the wave, respectively. Retaining terms up to first order in perturbation in Eqs. (7)–(11), the following equations are generated:

$$\begin{aligned} &\left[\omega - D_{e\perp}L_m - Z + P_e + b_{e\perp}\left((L_0 V) + \frac{\partial V}{\partial r}\frac{\partial}{\partial r}\right)\right. \\ &\quad + \frac{b_{e\perp}}{2e}\left((L_0 T_e) + \frac{\partial T_e}{\partial r}\frac{\partial}{\partial r}\right) - \frac{b_{e\perp}}{e}\frac{\partial T_e}{\partial r}\frac{\partial}{\partial r} \\ &\quad \left. + imb_{e\perp}\alpha_e \frac{1}{r}\frac{\partial V}{\partial r}\right] n_1 - \left[-b_{e\perp}\left(nL_m + \frac{\partial n}{\partial r}\frac{\partial}{\partial r}\right)\right. \\ &\quad \left. - q_e + imb_{e\perp}\alpha_e \frac{1}{r}\frac{\partial n}{\partial r}\right] V_1 = 0, \\ &\left[\omega - D_{i\perp}L_m - Z + P_i - b_{i\perp}\left((L_0 V) + \frac{\partial V}{\partial r}\frac{\partial}{\partial r}\right)\right. \\ &\quad \left. + imb_{i\perp}\alpha_i \frac{1}{r}\frac{\partial V}{\partial r}\right] n_1 - \left[b_{i\perp}\left(nL_m + \frac{\partial n}{\partial r}\frac{\partial}{\partial r}\right) - q_i\right. \end{aligned} \tag{13}$$

$$+imb_{i\perp}\alpha_i\frac{1}{r}\frac{\partial n}{\partial r}\Big]V_1=0, \tag{14}$$

where

$$L_m=\frac{1}{r}\frac{\partial}{\partial r}r\frac{\partial}{\partial r}-\frac{m^2}{r^2},$$

$$L_0=\frac{1}{r}\frac{\partial}{\partial r}r\frac{\partial}{\partial r},$$

$$P_e=D_ek^2+b_e\frac{\partial^2 V}{\partial z^2}+ikb_e\frac{\partial V}{\partial z},$$

$$P_i=D_ik^2-b_i\frac{\partial^2 V}{\partial z^2}-ikb_i\frac{\partial V}{\partial z},$$

$$q_e=-b_enk^2+ikb_e\frac{\partial n}{\partial z},$$

$$q_i=b_ink^2-ikb_i\frac{\partial n}{\partial z},$$

Now to obtain a dispersion relation, it is necessary to solve Eqs. (13) and (14). But it is difficult to do so analytically as mentioned earlier. Hoh[1] has suggested a dimensional treatment in this situation. Also, by applying variational analysis to solve the problem, he has shown that the results obtained by dimensional treatment are qualitatively in good agreement with what are predicted by the variational method. In the present situation, the differential operators, while acting on the parameters except V and T_e in Eqs. (13) and (14), are replaced by the scale factors as mentioned explicitly in Hoh's[1] paper. The scalings in the cases of V and T_e are only mentioned in this paper afterwards. The following assumptions are incorporated in the present analysis:

(a) q_i and p_i are neglected in the long-wavelength limit.

(b) The steady-state density distribution (n) is taken to be $J_0(\beta_{01}r/R)\cos(\pi z/L_z)$, where β_{01} is the first root of the zero-order Bessel function, R the plasma radius, and $L_z \gg L$, L being the length of the plasma column.

(c) The radial dependence of the perturbations (n_1 and V_1) is taken as $J_m(\beta_{m1}r/R)$, where β_{m1} is the first root of the mth-order Bessel function. It is found[1] that it is easier to excite such modes (for $m \leqslant 4$) having no nodes within a scale of magnitude R than the modes having nodes within that scale size.

(d) $\alpha_e/\alpha_i \gg 1$ and $b_{i\perp}/b_{e\perp} > 1$.

(e) $(kR\alpha_e)^2/m\beta_{01}C_m \ll 1$ (C_m being defined later) in the long-wavelength limit and at low magnetic fields. Instead of this assumption, Hoh[1] assumed $(\pi R/L_z)^2\alpha_e/2m \ll 1$ which does not hold for $m=0$ and therefore no inference can be made for the rotationally symmetric mode from Hoh's[1] analysis.

Next, with the scalings as done by Hoh[1] and the above assumptions, the general dispersion relation (for $m \geqslant 0$) is obtained from Eqs. (13) and (14) as

$$\begin{aligned}\omega=\frac{1}{A_1}\Bigg(&-\frac{\alpha_e b_{e\perp}}{R}\Bigg\{\Bigg[\eta\left(\frac{1}{\alpha_e}+\frac{y}{\alpha_i}\right)+mC_m\Bigg]B_1\\&+\frac{my\alpha_i}{C_m}A_1-mF_1\Bigg\}\frac{\overline{\partial V}}{\partial r}+\frac{\chi}{R}\frac{b_{e\perp}}{e}(A_1+B_1)\frac{\overline{\partial T_e}}{\partial r}\\&-(A_1+B_1)\overline{D}_ek^2+\overline{Z}\Bigg[A_1+\left(1-\frac{\alpha_e b_{e\perp}y}{\alpha_i b_{i\perp}}\right)B_1\Bigg]\\&+kb_eF_1\frac{\overline{\partial V}}{\partial z}-\frac{\beta_{m1}^2}{R^2}\Bigg[A_1+\left(1-\frac{\alpha_e\Phi_i y}{\alpha_i\Phi_e}\right)B_i\Bigg]\overline{D}_{e\perp}\Bigg)\\&+\frac{i}{A_1}\Bigg\{-[\eta b_{i\perp}F_1+m\alpha_e b_{e\perp}(A_1+(1-y)B_1)]\frac{1}{R}\frac{\overline{\partial V}}{\partial r}\\&+\frac{\chi}{R}\frac{b_{e\perp}}{e}F_1\frac{\overline{\partial T_e}}{\partial r}-F_1\overline{D}_ek^2-(A_1+B_1)kb_e\frac{\overline{\partial V}}{\partial z}\\&-\frac{\beta_{m1}^2}{R^2}F_1(\overline{D}_{e\perp}-D_{i\perp})\Bigg\},\end{aligned} \tag{15}$$

where

$$C_m=\frac{1}{m}\left(\beta_{m1}+\frac{\beta_{m1}^2}{\beta_{01}}\right),$$

$$\chi=\beta_{m1}-\tfrac{1}{2}\zeta,$$

$$A_1\approx C_m^2b_{i\perp}^2,$$

$$B_1=\alpha_ib_{i\perp}\left((\alpha_ib_{i\perp}-\alpha_ib_{i\perp}b)+\frac{\pi kb_eR^2}{m\beta_{01}L_z}\right),$$

$$F_1\approx C_m\left(b_{e\perp}b_{i\perp}\alpha_e-\frac{\pi kb_eb_{i\perp}R^2}{m\beta_{01}L_z}\right),$$

$$y=1-\frac{\pi k\alpha_eR^2}{m\beta_{01}L_z},$$

$$\phi_e=T_e/e,\quad \phi_i=T_i/e.$$

In deducing the above expression, specific distributions of T_e and V have not been incorporated as has been done for n [assumption (b)]. Here the following substitutions have been introduced:

$$\begin{aligned}\overline{L_0T_e}+\frac{\beta_{m1}}{R}\frac{\overline{\partial T_e}}{\partial r}&\rightarrow\frac{\zeta}{R}\frac{\overline{\partial T_e}}{\partial r},\\ \overline{L_0V}+\frac{\beta_{m1}}{R}\frac{\overline{\partial V}}{\partial r}&\rightarrow\frac{\eta}{R}\frac{\overline{\partial V}}{\partial r},\end{aligned} \tag{16}$$

where ζ and η are the scale constants to be determined from the experimental observation of the distributions of T_e and V, respectively. Here, the contributions from the second-order derivatives have been absorbed in the first-order derivative term. When the gradients of electron temperature and potential are almost constant, as are generally observed, the contribution from the second-order derivative term is negligible. But, otherwise, for an irregular distribution of T_e and V, an average value of the gradients has to be estimated.

In Eq. (15) the bars denote average of the parameters over the plasma volume.

B. Rotationally symmetric mode ($m=0$)

In the limit $m\to 0$ the general dispersion relation, Eq. (15), reduces to

$$\omega=\left[\bar{Z}+\frac{\chi}{R}\frac{b_{e\perp}}{e}\frac{\overline{\partial T}_e}{\partial r}+\frac{\eta}{R}\left(\frac{\pi kR^2}{2\beta_{01}^2L_z}\right)^2\frac{b_e^2}{b_{i\perp}}\frac{\overline{\partial V}}{\partial r}-\bar{D}_e k^2\right.$$

$$-\frac{\pi k^2R^2}{2\beta_{01}^2L_z}\frac{b_e^2}{b_{i\perp}}\frac{\overline{\partial V}}{\partial z}-\frac{\beta_{01}^2}{R^2}(\bar{\Phi}_e+\Phi_i)b_{e\perp}$$

$$\left.-\left(\frac{\pi kb_eR}{2\beta_{01}L_z\,b_{i\perp}}\right)^2D_{i\perp}\right]+i\left[\frac{\pi k}{2L_z}\frac{b_e}{b_{i\perp}}(\bar{D}_{e\perp}-\mathbf{D}_{i\perp})\right.$$

$$\left.+\frac{\pi kb_eR}{2\beta_{01}^2L_z}\left(\eta\frac{\overline{\partial V}}{\partial r}-kb_e\frac{\overline{\partial V}}{\partial z}\right)\right]. \tag{17}$$

Here the terms involving the production, the positive temperature gradient, and the radial electric field parallel to the density gradient are destabilizing while the diffusion terms are stabilizing. So the $m=0$ mode instability will grow when

$$\left[\frac{\eta}{R}\left(\frac{\pi kR^2}{2\beta_{01}^2L_z}\right)^2\frac{b_e^2}{b_{i\perp}}\frac{\partial\bar{V}}{\partial r}+\bar{Z}+\frac{\chi}{R}\frac{b_{e\perp}}{e}\frac{\partial\bar{T}_e}{\partial r}\right]$$
$$\geq\left[\bar{D}_ek^2+\frac{\beta_{01}^2}{R^2}(\bar{\Phi}_e+\Phi_i)b_{e\perp}+\left(\frac{\pi kRb_e}{2\beta_0L_zb_{i\perp}}\right)^2D_{i\perp}\right.$$
$$\left.+\frac{\pi k^2R^2}{2L_z\beta_{01}^2}\frac{b_e^2}{b_{i\perp}}\frac{\partial\bar{V}}{\partial z}\right] \tag{18}$$

and its frequency of oscillation will correspond to the imaginary part of Eq. (17). Here a positive temperature gradient is found to have a significant role in exciting the $m=0$ mode as is indicated in the third term on the left-hand side of Eq. (18). The term involving $D_{i\perp}$ (18) is very small for a long Penning device (as in the present case) and it can be neglected. The steady-state parameters in the above expression are analyzed in Sec. II D.

C. Mode $m\neq 0$

For the $m\neq 0$ modes, $y\approx 1$ and the dispersion relation, Eq. (15), reduces to the following form:

$$\omega=\frac{1}{A_1}\left\{-\frac{\alpha_eb_{e\perp}}{\alpha_i}\{[\eta+(1+\alpha_i)mC_m]B_1\}\frac{1}{R}\frac{\overline{\partial V}}{\partial r}\right.$$

$$+\frac{\chi}{R}\frac{b_{e\perp}}{e}(A_1+B_1)\frac{\overline{\partial T}_e}{\partial r}-(A_1+B_1)\bar{D}_ek^2$$

$$+\bar{Z}\left[A_1+\left(1-\frac{\alpha_eb_{e\perp}}{\alpha_ib_{i\perp}}\right)B_1\right]+kb_eF_1\frac{\overline{\partial V}}{\partial z}$$

$$\left.-\frac{\beta_{m1}^2}{R^2}\left[A_1+\left(1-\frac{\alpha_e\Phi_i}{\alpha_i\bar{\Phi}_e}\right)B_1\right]\bar{D}_{e\perp}\right\}$$

$$+\frac{i}{A_1}\left[-(\eta b_{i\perp}F_1+m\alpha_eb_{e\perp}A_1)\frac{1}{R}\frac{\overline{\partial V}}{\partial r}+\frac{\chi}{R}\frac{b_{e\perp}}{e}F_1\frac{\overline{\partial T}_e}{\partial r}\right.$$

$$\left.-F_1\bar{D}_ek^2-(A_1+B_1)kb_e-\frac{\overline{\partial V}}{\partial z}-\frac{\beta_{m1}^2}{R^2}F_1(\bar{D}_{e\perp}-D_{i\perp})\right]. \tag{19}$$

Here the growth condition is a manifestation of the competition between the terms involving the radial electric field, the temperature gradient, the production, and the diffusion. A positive temperature gradient is found to have a destabilizing influence in this situation also. However, in the previous works[1,2] the effect of the temperature gradient was ignored and only the radial electric field and the density gradient were considered.

D. Steady-state parameters for a long Penning discharge

Hoh[1] has explicitly calculated the expressions for Z, $\partial V/\partial r$, and $\partial V/\partial z$ for a Penning configuration. In the present situation, by also incorporating the effect of the temperature gradient the relevant parameters are determined following the aforesaid calculation and these follow:

$$\bar{Z}=\frac{b_i}{b_e}\frac{I}{\bar{n}e\pi R^2L}+\left(\frac{\pi}{L_z}\right)^2\bar{D}_a,$$

$$\frac{\partial\bar{V}}{\partial r}+\frac{1}{2e}\frac{\partial\bar{T}_e}{\partial r}$$

$$=-\bar{\Phi}_e\frac{\beta_{01}}{R}+\frac{I}{2\pi RL\bar{n}eb_{e\perp}}-\frac{R}{2}\left(\frac{\pi}{L_z}\right)^2\frac{\bar{D}_a}{b_{e\perp}}, \tag{20}$$

$$\frac{\overline{\partial V}}{\partial z}\approx-\frac{\pi}{L_z}\bar{\Phi}_e,\qquad \bar{D}_a=\frac{\bar{D}_eb_i+D_ib_e}{b_e+b_i},$$

where I is the discharge current, $\bar{D}_a$ is the average parallel (to $\mathbf{B}$) ambipolar diffusion coefficient, and $\bar{n}$ is the average density of the charged particles.

The above expressions together with Eqs. (17) and (19) are utilized to determine the growth condition and the frequency of oscillation of the $m=0$ and $m\neq 0$ waves.

III. EXPERIMENTAL RESULTS AND DISCUSSION

Here the discharge is initiated in a cold-cathode Penning device shown schematically in Fig. 1. Two Al cathodes (K) of diameter 1.8 cm are separated by 47 cm and the hollow cylindrical anodes (A) are of diameter 2 cm, and length 2 cm, the closest anode-cathode separation being 5 mm. There are two grid structures (G), each in front of an

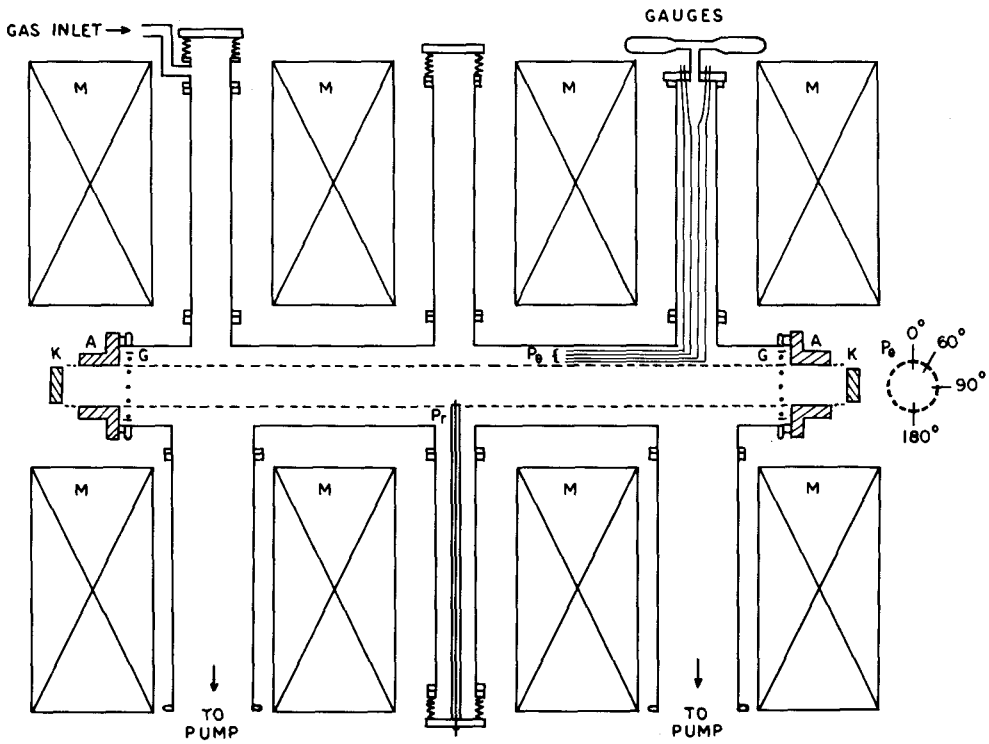

FIG. 1. Schematic diagram of the experimental arrangement; P_r: radially movable Langmuir probe; P_θ: azimuthal probe assembly; M: magnet coils; dotted horizontal lines: the plasma boundary.

anode, as shown, at a separation of ~ 3 mm. Here the grid assembly has approximately 80% transparency. The radial steady-state distributions of the plasma parameters are measured by a radially movable Langmuir probe (P_r) and the azimuthmal mode number of the waves are determined by monitoring the signals at a number of azimuthal probes (P_θ, inserted in Fig. 1), all of which are placed at a particular radial and axial location. In the present experiment nitrogen gas has been used.

When the grids are floating, at high gas pressure ($p \sim 10^{-2}$ Torr) a strong rotationally symmetric mode is observed to be excited at low magnetic fields ($B \leqslant 350$ G). The rotational symmetry is concluded by observing zero phase shift between the signals appearing at the azimuthal probes separated at several angles (30°, 60°, 90°, 150°, and 180°). A typical example has been cited in Fig. 2, photographed on a dual-trace oscilloscope. When the grids are connected to the anodes, the above oscillations disappear. Thus the $m=0$ mode instability is suppressed.

To acknowledge the driving agents of this instability, the steady-state distributions of the plasma parameters (n_i, V_F and T_e) are measured for the two situations: when

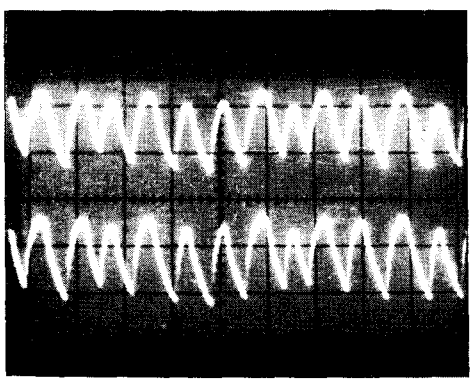

FIG. 2. An example of the oscillations at two azimuthal probes separated by 90° (sweep speed 0.5 msec/cm), the pattern being same for other azimuthal separations. All the probes are kept at a radial location $r \approx 1$ cm.

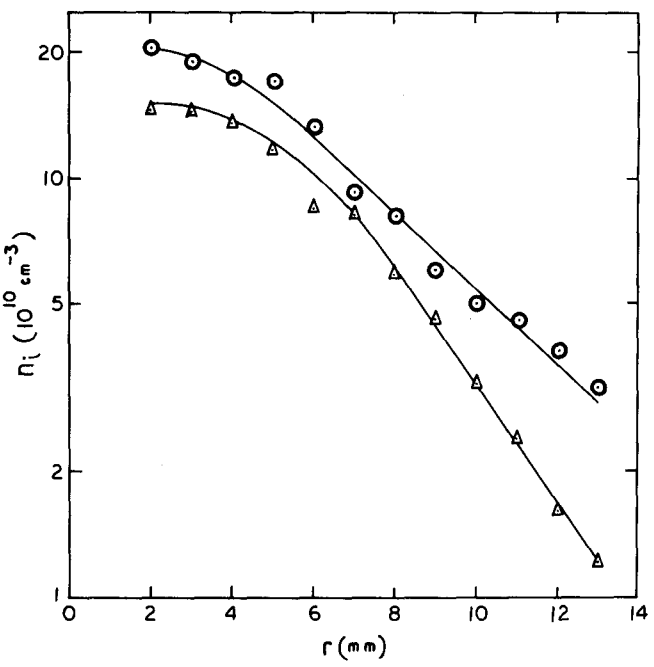

FIG. 3. Radial ion density (n_i) distributions for nitrogen: ⊙ for grids floating and △ for grids connected to anodes. r denotes radial position of the probe. Gas pressure is 3×10^{-2} Torr; discharge current is 30 mA; and magnetic field is 280 G.

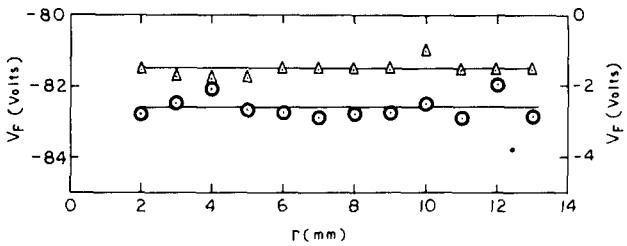

FIG. 4. Radial floating potential (V_F) distributions: ⊙ for grids floating and △ for grids connected to anodes, the discharge conditions being the same as in Fig. 3. Ordinate scale: left side for ⊙; right side for △.

the grids are floating and when these are connected to the anodes. An example of these distributions are shown in Figs. 3–5 for a typical relevant situation. The average radial electric field in the plasma is estimated from the floating potential and the electron-temperature distributions since the estimation of the electric field from the plasma potential (V_s) distribution may be in error in the presence of magnetic fields. It is found from the observed distributions (Figs. 4 and 5) that the radial electric field and the temperature gradient that exist while the grids are floating become inappreciable when the grids are connected to the anodes. In the density distribution (Fig. 3), it is found that when the grids are connected to the anodes, there is nearly a 20% reduction of n_i in the production region (near the axis) and almost 50–60% reduction in the outer diffusional region. These observations can be explained qualitatively as follows.

The gradients of the plasma potential and the electron temperature are related to the radial transport through the following equation:

$$\frac{\partial V}{\partial r}+\frac{1}{2e}\frac{\partial T_e}{\partial r}=-\Phi_e\frac{1}{n}\left|\frac{\partial n}{\partial r}\right|+\frac{v_{er}}{b_{e\perp}}. \tag{21}$$

According to the present observation, the radial flux of the particles is reduced when the grids are connected to the anodes and this causes a reduction of the gradients of T_e and V. This is in agreement with the Eq. (21). Thus the grids have suppressed the observed instability by reducing the gradients of T_e and V and also increasing the radial confinement of the particles.

The above experimental observation reveals the underlying truth of the mechanism of the present instability. For further justification of this instability, the theoretical model, as enumerated in Sec. II, is next studied in light of the present discharge condition. In this context, the oscillation frequency of an $m=0$ mode instability and also the role of the various driving agents for its excitation are estimated below.

Here, in determining the scaling parameters η and ζ [as mentioned in Eq. (16)], the distributions of V and T_e are required. However, the distribution of the plasma potential (V) is found out from those of the floating potential (V_F) and the electron temperature (T_e) following the relationship[14]

$$V=V_F+(4/e)T_e, \tag{22}$$

in the case of nitrogen. In the present observations, as shown in Fig. 4, the floating potential is practically independent of the radial locations. So it can be inferred from Eq. (22) that the distribution of V, in the present situation, is akin to that of T_e and consequently

$$\frac{\overline{\partial V}}{\partial r}=\frac{4}{e}\frac{\overline{\partial T_e}}{\partial r} \quad \text{and} \quad \eta=\zeta. \tag{23}$$

Further, Fig. 5 indicates that $\partial T_e/\partial r$ is not constant. So, here in estimating $\overline{\partial T_e}/\partial r$ and ζ, it is necessary to choose an analytic expression which approximately explains the general feature of the present T_e distribution. A distribution of the type $T_{eR}\exp\{-[(r-R)/R]^2\}$, where T_{eR} is the electron temperature at $r=R$ (here at $r=1$ cm), is illustrative of the present situation (Fig. 5). Although it is an approximate choice of the experimental distribution, it does by no means annihilate the essence of the present investigation. Now it is evident from the density distribution in Fig. 3 that the production region (plasma core) extends from the axis to $r<0.6R$ ($R=1$ cm) and the region beyond it is diffusion controlled. In general, the gradients have a significant role in the diffusional region of a plasma. The average values of $\partial T_e/\partial r$ and ζ are determined by averaging the respective quantities in the diffusional region which in the present experimental situation is given by $0.6R\leqslant r\leqslant R$. Now taking $T_{eR}=1.8$ eV (Fig. 5) it is found that

$$\frac{\overline{\partial T_e}}{\partial r}=1.1\ \frac{\text{eV}}{\text{cm}} \quad \text{and} \quad \frac{\overline{\partial V}}{\partial r}=4.4\ \frac{\text{V}}{\text{cm}}$$

[Eq. (23)],

$\zeta=0.5$, $\eta=0.5$, $\chi=2.15$ (for the mode $m=0$).

The other parameters in the present situation ($p=3\times10^{-2}$ Torr, $B=280$ G, and $I=30$ mA) are as follows:

$\bar{\Phi}_e=1.2$ (Fig. 5), $\Phi_i\approx0.1$

(as usually taken in a cold plasma),

$\alpha_e=\omega_e\tau_e=69$,

$\alpha_i=\omega_i\tau_i\approx0.28$ (τ's being determined as Ref. 15),

$b_e=2.5\times10^7$, $b_i=1.01\times10^5$,

$b_{e\perp}=5.25\times10^3$, $b_{i\perp}=1.37\times10^4$,

$\bar{D}_e=3.0\times10^7$, $D_i=1.01\times10^4$,

$\bar{D}_{e\perp}=6.3\times10^3$, $D_{i\perp}=9.37\times10^3$,

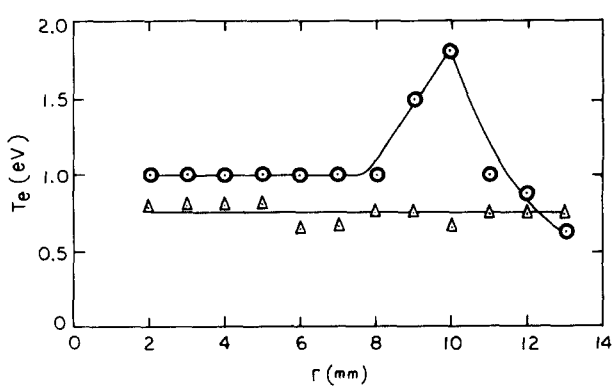

FIG. 5. Radial electron temperature (T_e) distributions: ⊙ for grids floating and △ for grids connected to anodes, the discharge conditions being the same as Fig. 3.

where the Φ's are in V, the b's in cm^2/V sec, and the D's in cm^2/sec. The production rate Z is estimated from Eq. (20). Now taking $k \approx \pi/L_z$ (where $L_z = 2L$, Hoh[1]) and using the above numerical values of the discharge parameters, the oscillation frequency for the fundamental wave of the $m=0$ mode instability, as estimated from the imaginary part of Eq. (17), is nearly 6 kHz, while it is experimentally observed to be nearly 3 kHz (Fig. 2). Further, from the growth criterion (18) it is found that the terms containing the temperature gradient and the potential gradient are the main driving factors for exciting the $m=0$ mode instability. Introducing the numerical values as indicated above, it is found from Eq. (18) that

$$\frac{\text{Term containing temperature gradient}}{\text{Term containing potential gradient}} \approx 90 \qquad (24)$$

in the present situation. Moreover, the critical value of the temperature gradient for the growth of the $m=0$ mode is estimated to be nearly 6 eV/cm, while experimentally it is found to be nearly 1.1 eV/cm.

The above numerical estimates suggest that the results obtained from the dimensional analysis of the present problem are in satisfactory agreement with the experimental observations. The comparatively larger departure of the experimentally observed critical temperature gradient (1.1 eV/cm) from the theoretically predicted value (6 eV/cm) does not negate the appreciation of the present model based on the dimensional treatment, since a linear analysis only reveals the possibility of the growth of the instability but can not determine the threshold values exactly as nonlinear contributions become important in this concern. Moreover, the dimensional treatment is utilized to appreciate a qualitative picture of a complicated problem. So, such a model can be adopted reasonably if the results derived from it are in an order-of-magnitude agreement with those obtained experimentally. Even a very close agreement between such a theoretical model and the experimental observations may be often fortuitous. Finally, it is also found from the present theoretical analysis that the temperature gradient has the predominant destabilizing influence [being nearly two orders of magnitude higher than the influence of potential gradient, Eq. (24)] in the present concern. Therefore, the physical mechanism for the onset of the $m=0$ mode instability can be attributed to the radial electron-temperature gradient. Experimental observations concerning the excitation and the stabilization of the $m=0$ mode, as reported in the present paper, also reveal the same fact.

IV. CONLUSIONS

In the present problem a general theoretical framework of the low-frequency instability driven by radial density, potential, and electron temperature gradients has been enumerated. In the earlier works by Hoh,[1] Bingham,[2] etc., the effect of the electron-temperature gradient has not been taken into account. Here this effect (electron-temperature gradient) has been found to be very important in understanding the observed $m=0$ mode in a PIG device. In the analysis given by Hoh,[1] the possibility of the occurrence of the $m=0$ mode has been ignored. The present theory is also capable of determining the growth condition and the frequency of the $m \neq 0$ wave in a general situation.

From both the experimental and the theoretical investigations in the present situation it is found that an $m=0$ mode instability can occur in a PIG device when there exists a positive electron-temperature gradient along with the density gradient. Detailed experimental studies regarding the occurrence and the radial dependence of this $m=0$ mode and also of the higher modes are in progress and will be reported later.

ACKNOWLEDGEMENTS

The authors acknowledge their gratitude to Professor D.N. Kundu for supporting the present work and to Professor S.K. Mukherjee for encouragement. Authors are also thankful to Dr. J. Basu for many helpful discussions.

[1]F.C. Hoh, Ark. Fys. **24**, 285 (1963).
[2]R. Bingham, Phys. Fluids **7**, 1001 (1964).
[3]K.I. Thomassen, Phys. Fluids **9**, 1836 (1966).
[4]E.B. Hooper, Jr., Plasma Phys. **12**, 855 (1970).
[5]M.G. Kaganskii, D.L. Kaminskii, and A.N. Klyucharev, Sov. Phys.-Tech. Phys. **9**, 815 (1964).
[6]B.B. Kadomtsev, Nucl. Fusion **1**, 286 (1961).
[7]G. Ecker, W. Kröll, and O. Zöller, Proc. 6th Intern. Conf. Ionized Phenomena Gases, Paris, 1963, Vol. 1, p. 405 (unpublished).
[8]F.F. Chen, Phys. Rev. Lett. **8**, 234 (1962).
[9]G. Horikoshi, T. Kuroda, K. Matsuura, A. Miyahara, M. Masuzaki, and S. Nagao, Proc. 8th Intern. Conf. Ionized Phenomena Gases, Vienna, 1967, p. 550 (unpublished).
[10]A.B. Mikhailovskii, in *Advances in Plasma Physics* 5, edited by A. Simon and W.B. Thompson (Wiley, New York, 1974), p. 121.
[11]L. Pekárek and V. Krejčí, Czech. J. Phys. B **12**, 815 (1962).
[12]F. Klan, Proc. 9th Intern. Conf. Ionized Phenomena Gases, Bucharest, 1969, p. 246 (unpublished).
[13]S.I. Braginskii, in *Reviews of Plasma Physics* 1, edited by M.A. Leontovich (Consultants Bureau, New York, 1965), pp. 205–311.
[14]R. Bingham, F.F. Chen, and W.L. Harries, Princeton Univ. Plasma Phys. Lab. Report MATT-63, 1962 (unpublished).
[15]S.C. Brown, *Basic Data of Plasma Physics* (Wiley, New York, 1959).